



# Effects of shear work on non-equilibrium heat transfer characteristics of rarefied gas flows through micro/nanochannels



Mojtaba Balaj, Ehsan Roohi\*, Hassan Akhlaghi

High Performance Computing (HPC) Laboratory, Department of Mechanical Engineering, Ferdowsi University of Mashhad, P.O. Box 91775-1111, Mashhad, Iran

## ARTICLE INFO

### Article history:

Received 1 August 2014

Received in revised form 14 November 2014

Accepted 27 November 2014

### Keywords:

Viscous dissipation

Constant wall heat flux

Counter gradient heat flux

Nusselt number singularity

## ABSTRACT

In the current work, the effect of shear work due to the velocity slip on the non-equilibrium heat transfer in a pressure driven micro/nanochannel is evaluated under the constant wall heat flux boundary condition. As our simulation tool, the DSMC method is employed. Implementation of the wall heat flux in the DSMC method is performed using the “modified iterative” technique. We investigate the effects of rarefaction, property variations and compressibility. The numerical results show that shear stress on the walls significantly affects all aspects of the flow behavior and heat transfer through micro/nanochannels such as heat flux rates. We also analyze the counter-gradient heat flow (cold to hot heat transfer) phenomenon appearing at the cooling conditions. It is observed that viscous dissipation affects the heat flux applied to the walls and may overcome the wall heat flux, i.e., in the case of low cooling wall heat flux condition, shear work may completely heat the flow field. Nusselt number singularity is also discussed.

© 2014 Elsevier Ltd. All rights reserved.

## 1. Introduction

With today's rapid development of micro/nano devices, optimum design and prediction of fluid and heat transfer characteristics of rarefied gas flow through micro/nano-devices are crucial. As the size of systems falls in the order of mean free path of gas molecules ( $\lambda$ ), the effects of properties variation, viscous dissipation and flow rarefaction influence the fluid flow and heat transfer behaviors. The viscous dissipation and flow rarefaction are characterized by Brinkman number ( $Br = \mu u_b^2 / 2Hq_w$ ) and Knudsen number ( $Kn = \lambda/H$ ), respectively. Compared to the macro-devices, the viscous dissipation due to a large surface to volume ratio causes a measurable increase in the heat transfer rate at solid boundaries.

An essential characteristic of the heat transfer behavior of any system is the Nusselt number (Nu), defined as the ratio of the convective heat transfer coefficient to the conductive heat transfer coefficient across the boundary. For a parallel plate channel subject to constant wall heat flux (CWH) boundary condition, the Nusselt number could be written as follows:

$$Nu = \frac{2q_w H}{k_t(T_w - T_b)} \quad (1)$$

where  $q_w$ ,  $H$ ,  $k_t$  and  $T_w$  are the wall heat flux, the channel height, gas thermal conductivity and wall temperature, respectively. Moreover, the bulk temperature ( $T_b$ ) is defined as

$$T_b = \frac{\int_A \rho u_x T dA}{\int_A \rho u_x dA} \quad (2)$$

There are theoretical and numerical investigations around the topic of heat transfer in micro/nano rectangular channels in low to moderate Knudsen number ranges, i.e., slip flow regime. Inman [1] has performed the first investigation of slip flow heat transfer. Inman studied a parallel plate channel with constant wall heat flux analytically. He studied the velocity slip and temperature jump in his investigation and proposed an expression for the Nusselt number as a function of rarefaction (Kn) parameter. Hooman [2] suggested a correlation using the superposition approach for straight microchannels of uniform, but with an arbitrary cross section in the slip region. He showed that applying an average slip velocity and temperature jump definition; one can still use the no-slip/no-jump results with some minor modifications. Miyamoto et al. [3] studied heat transfer characteristics of the choked gas flows through a narrow parallel-plate channel. They found that due to the developing flow effects, the Nusselt number abruptly changes near the inlet and exit. In addition to viscous dissipation and rarefaction effects, the influence of streamwise conduction was investigated by Jeong and Jeong [4] on the Graetz problem in a flat plate microchannel. This investigation revealed that the Nusselt number decreases as the Peclet number decreases. They also showed that if the streamwise conduction is included, the Nusselt number becomes greater compared with the solution where streamwise conduction is neglected. The interactive effects of the Brinkman and Knudsen numbers on the Nusselt number are analytically

\* Corresponding author. Tel.: +98 51 38805136; fax: +98 51 38763304.

E-mail address: [e.roohi@ferdowsi.um.ac.ir](mailto:e.roohi@ferdowsi.um.ac.ir) (E. Roohi).

determined by Aydin and Avci [5]. They showed that an increase in the Knudsen number decreases the Nusselt number due to the increased temperature jump over the wall. They indicated that in the absence of viscous dissipation, the solution is independent of whether there is wall heating or cooling. The effects of viscous dissipation and rarefaction on hydrodynamically and thermally developed laminar forced convection of constant wall heat flux (CWH) microchannel was considered by Sadeghi and Saidi [6]. They showed that the effect of viscous heating on the Nusselt number at greater values of the Knudsen number becomes insignificant and in the absence of viscous heating, increasing values of Knudsen number lead to smaller values of the Nusselt number. Furthermore, they observed that viscous heating causes singularities in the Nusselt number values. These singularities have been discussed by Miyamoto et al. [3], Aydin and Avci [5] and Sheela-Francisca and Tso [7] as well. Hadjiconstantinou [8] considered the effect of shear work at solid boundaries on the convective heat transfer and obtained the solution of the constant-wall-heat-flux problem in small scale gaseous flows where slip effects are present. Colin [9] provided a detailed review of the convective heat transfer in microchannels with different geometrical shape and wall boundary conditions. His study was focused on flows with  $Kn < 0.2$ . A comparison of different models for Nusselt number showed that there is a considerable difference between different analytical Nusselt expressions.

Even though previous researchers have studied the effects of viscous dissipation, but some simplifications made in analytical/numerical solutions caused that the physics behind the heat transfer was not predicted correctly in particular cases. For example, in some occasions, it was assumed that the wall temperature gradient is constant and equal to the bulk temperature gradient along the channel, i.e.,  $\partial T_w / \partial x = \partial T_b / \partial x = const.$ , i.e., see Ref. [8]. This assumption makes prediction of the Nusselt number singularity impossible. Moreover, if the flow properties variation and compressibility effects are neglected [2,5,8], it is expected that the derived expressions for any flow properties such as Nusselt number and temperature profile become valid only for low dissipation rates, i.e., small Brinkman numbers. The objective of the present work is to numerically investigate the effects of rarefaction and viscous dissipation on the convective heat transfer behaviour of parallel plate micro/nanochannels in the slip flow regime, subject to constant wall heat flux thermal boundary condition. In this study, the order of magnitude of the shear stresses, slip velocity and viscous dissipation have been investigated numerically for specific cases. In this way, improvement of analytical solutions with the help of numerical analysis would be possible. A detailed discussion of the contrast between cooling heat flux and viscous dissipation, which eventually leads to the singularity in Nusselt number, is presented. Numerical results are obtained using a two-dimensional direct simulation Monte Carlo (DSMC) solver. To verify the simulations, numerical results for thermally and hydrodynamically fully developed parallel plate under constant wall heat flux for Nusselt numbers are compared with different analytical solutions which account viscous dissipation. We study the effect of shear work at the wall boundaries and consider how viscous dissipation affects convective heat transfer.

### 3. Numerical method

The present research uses the DSMC method that follows the scheme proposed by Bird [10]. It is a particle base method which utilizes random sampling for obtaining numerical solutions of rarefied gas flows. The method simulates the gas flow using many independent simulator particles which are representatives of a large number of real gas molecules. In order to implement DSMC,

the flow field must be divided into computational cells. Provided that an adequately large number of particles are used, and the cell size and time step are suitably small, the DSMC method converges to the solution of the Boltzmann equation. DSMC time step should be chosen small enough such that the positional changes of particles and their collisions could be decoupled for each time step. The cells provide geometric boundaries required to sample macroscopic properties. Each cell is typically divided into subcells utilized to increase the accuracy of the selection of collision pairs. In the current work, the previous code of Akhlaghi and co-workers [11–16] is extended to simulate rarefied flow in the micro/nano channel geometry. The GHS collision model, introduced by Hassan and Hash [17], is utilized to consider accurate variation of the viscosity with the temperature over a wide range of temperature variations. This model is an extension of the variable hard sphere (VHS) model to include terms that allow modeling of molecules with both repulsive and attractive potentials. For the GHS model, the total collision cross section could be written as follows:

$$\sigma = \sigma_0(\phi(g_0/g)^{2\nu_1} + (1 - \phi)(g_0/g)^{2\nu_2}) \quad (3)$$

where  $\sigma_0 = \pi d_0^2$  is the reference cross section,  $g = \sqrt{4RT}$  and the parameters with subscript zero are calculated at the reference temperature ( $T_0$ ), for more details, see Ref. [17]. The choice of the collision pair is done based on the no time counter (NTC) method. Monatomic argon,  $m = 6.63 \times 10^{-26}$  kg and  $d = 4.17 \times 10^{-10}$  m, is considered as the working fluid. In order to ensure the satisfaction of the limits on the cell size, the cell dimensions are considered as  $0.1\lambda$  and are much smaller than that for most cases. 30 particles are initially set in each cell to minimize the scattering noise. All walls are treated as diffuse reflectors using the full thermal accommodation coefficient. Half-range Maxwellian distribution is used to determine the velocity of the wall-reflected particles. After achieving steady flow condition, sampling of flow properties within each cell is fulfilled during a sufficient time period to suppress the statistical scatters of the solution. All thermodynamic parameters such as velocity, density, and temperature are then determined from this time-averaged data. The wall heat flux is imposed in the DSMC solver using the “modified iterative” technique developed. To impose a desired wall heat flux ( $q_{des}$ ) in the iterative technique previously suggested by Akhlaghi et al. [11], the wall temperature is corrected from the previous time step magnitude,  $T_w(x)^{old}$  according to the following formula:

$$T_w(x)^{new} = T_w(x)^{old} \left( 1 + RF \frac{q_w(x) - q_{des}(x)}{|q_{des}(x)| + \varepsilon_0} \right) \quad (4)$$

Adjusting the relaxation factor (RF) in a manner which ensures the convergence behavior depends on the desired wall heat flux magnitude, flow rarefaction (Kn), wall sampling period ( $\Delta t$ ) and number of DSMC particles impinging the wall. Therefore, it is difficult to determine an efficient value for RF in each case. The parameter  $\varepsilon_0$  which is defined only in the case of adiabatic condition is a non-zero positive value which is negligible compared to the incident energy

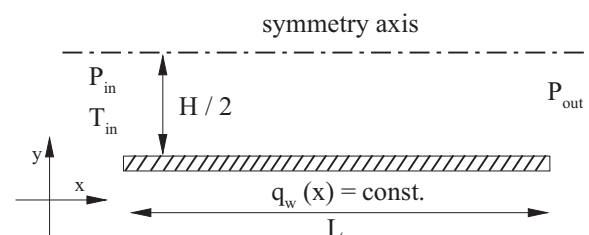


Fig. 1. 2D plane micro/nanochannel geometry and imposed boundary conditions.

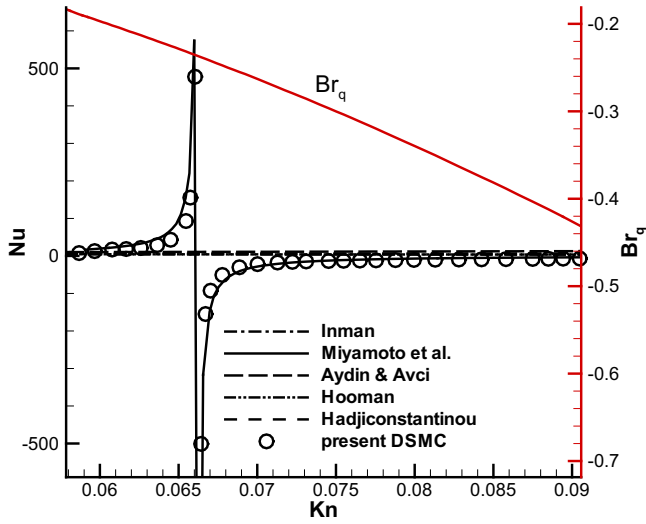


Fig. 2. Comparison of the Nusselt number of the DSMC solution with different analytical methods, Nu reaches an asymptotic value  $q_w = -25 \text{ W/cm}^2$ .

Table 1  
The fundamental parameters of investigated cases.

Case number	Wall heat flux, $q_w$ (W/cm <sup>2</sup> )	Inlet temperature, $T_{in}$ (K)	Pressure ratio (PR)
1	75	200	3
2	25	200	3
3	-25	400	3
4	-75	400	3

flux. In the “modified iterative” technique, the wall temperature is obtained as follows:

$$T_w(x)^{new} = T_w(x)^{old} \left( 1 + \frac{q_w(x) - q_{des}(x)}{(\dot{m}C_p T_{avg})/L} \right) \quad (5)$$

The modified iterative technique eliminates the need of using relaxation factor and  $\epsilon_0$ , as a result, it is easier to implement compared to Eq. (4). In the above equation,  $\dot{m}$ ,  $C_p$ ,  $T_{avg}$  and  $L$  are the mass flow rate, specific heat, average temperature of the flow, and the length of the wall, respectively. Our numerical experiences showed that

the convergence speed of the modified iterative technique is similar to the iterative technique.

To calculate the Nusselt number, the thermal conductivity of the gas is related to the gas viscosity as follows:

$$k = (15/4)(k/m)\mu \quad (6)$$

For GHS collision model, gas viscosity is computed according to the following relation [18]:

$$\mu = \frac{15\sqrt{\pi}}{16\Gamma(4 - \nu_1)} \frac{(T/T_0)^{0.5+\nu_1}}{(\phi + (1 - \phi)S_0(T_0/T)^{\nu_2-\nu_1})} \frac{mg_0}{\sigma_0} \quad (7)$$

For argon gas flow, Macrossan [18] showed that an accurate variation of the viscosity with the temperature could be obtained with  $\nu_1 = 2/13$ ,  $\phi = 0.61$  and  $\nu_2 = 4/13$ . Macrossan [18] showed that argon viscosity computed by the GHS model agrees well with the experimental data over a wide range of temperature. As the GHS model benefits from a molecular-based model which simulates the collisions correctly, it accurately considers the dependency of the viscosity on the temperature.

#### 4. On the validity of the theoretical solution

Fig. 1 shows the geometry of the 2D plane micro/nano channel and imposed boundary conditions at the inlet, outlet and walls.  $L$  and  $H$  are the channel length and height, respectively. It is heated/cooled symmetrically from walls. For validation purpose, we apply the modified iterative technique to impose the wall heat flux and compute the Nusselt number.

There is a wide set of analytical and numerical studies which investigated the heat transfer behavior of micro/nano systems. A main characteristic of heat transfer behavior of a system is the Nusselt number. Usually these studies obtained expressions for Nu number variations with the Knudsen number. Colin [9] provided a detailed comparison between the analytical expressions for Nu number in microchannels with different cross-sections. Fig. 2 compares our DSMC results for Nu number variations along a parallel plate microchannel subject to CWH equal to  $-25 \text{ W/cm}^2$  with four analytical relations for parallel plate channels. Dependency of heat conductivity on the temperature is considered to calculate the Nu number. The Br number variation versus Kn number is shown in this figure with a red line. Current DSMC solution is close to Miyamoto et al. result which considers the viscous dissipa-

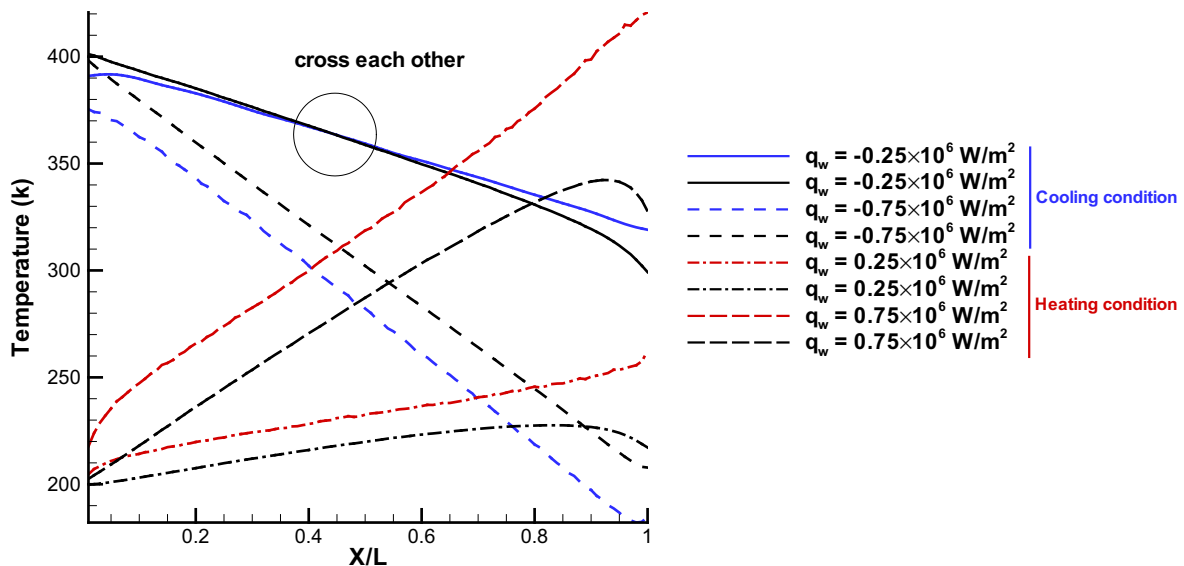


Fig. 3. The wall and bulk temperature variation along the channel for different wall heat fluxes.

tion suitably. DSMC and Miyamoto et al. results show singularity in Nusselt number while other analytical solutions cannot predict this singularity.

Miyamoto et al. [3] studied the effect of viscous heating in constant heat flux cases between parallel plates in the slip flow regime and obtained an expression for Nu as a function of Knudsen number and Brinkman number. In the case of full diffusive walls, their expression is as follows:

$$Nu = \left\{ \frac{9Br_0}{(1+6Kn)^2} \left[ \frac{3+42Kn+140Kn^2}{35(1+6Kn)} + \frac{4 \left( \frac{1.0618 \times 27}{7+1} \right) Kn^2}{Pr} \right] + \frac{17+168Kn+420Kn^2}{140(1+6Kn)^2} + \frac{1.0618 \times 27 Kn}{2Pr} \right\}^{-1} \quad \text{Eq. (20) of Ref. [3]} \quad (8)$$

Once the wall cooling is applied, the heat flux generated by the viscous dissipation may balance the effect of the wall cooling. Therefore, in the case of cooling condition, the analytical solutions are valid when they account viscous dissipation effects.

### 5. Results and discussion

In this section the results of heat transfer behavior for cases listed in Table 1 are presented. Both of cooling condition, i.e.  $q_w < 0$  and heating condition, i.e.  $q_w > 0$  is considered here. Our experiences on the channel flow [19] already indicated that the DSMC results do not depend on the aspect ratio (AR) of the micro-channel with  $AR \geq 20$ . Therefore, to balance the numerical cost and accuracy, we set channels' aspect ratio equal to 20.

Constant wall heat flux induces a temperature gradient into the channel walls and gas flow. Fig. 3 shows the wall and fluid bulk temperature distribution along the channel. The black lines correspond to the bulk temperature and color lines correspond to the wall temperatures. As is seen in this figure, in the case of heating condition, the walls heat the flow and the fluid bulk temperature increases along the channel. While cooling heat flux cools the flow and the fluid bulk temperature decrease along the channel. In the case of  $q_w = -25 \text{ W/cm}^2$ , the wall and bulk temperature lines cross each other. In the first section of the channel, the wall temperature

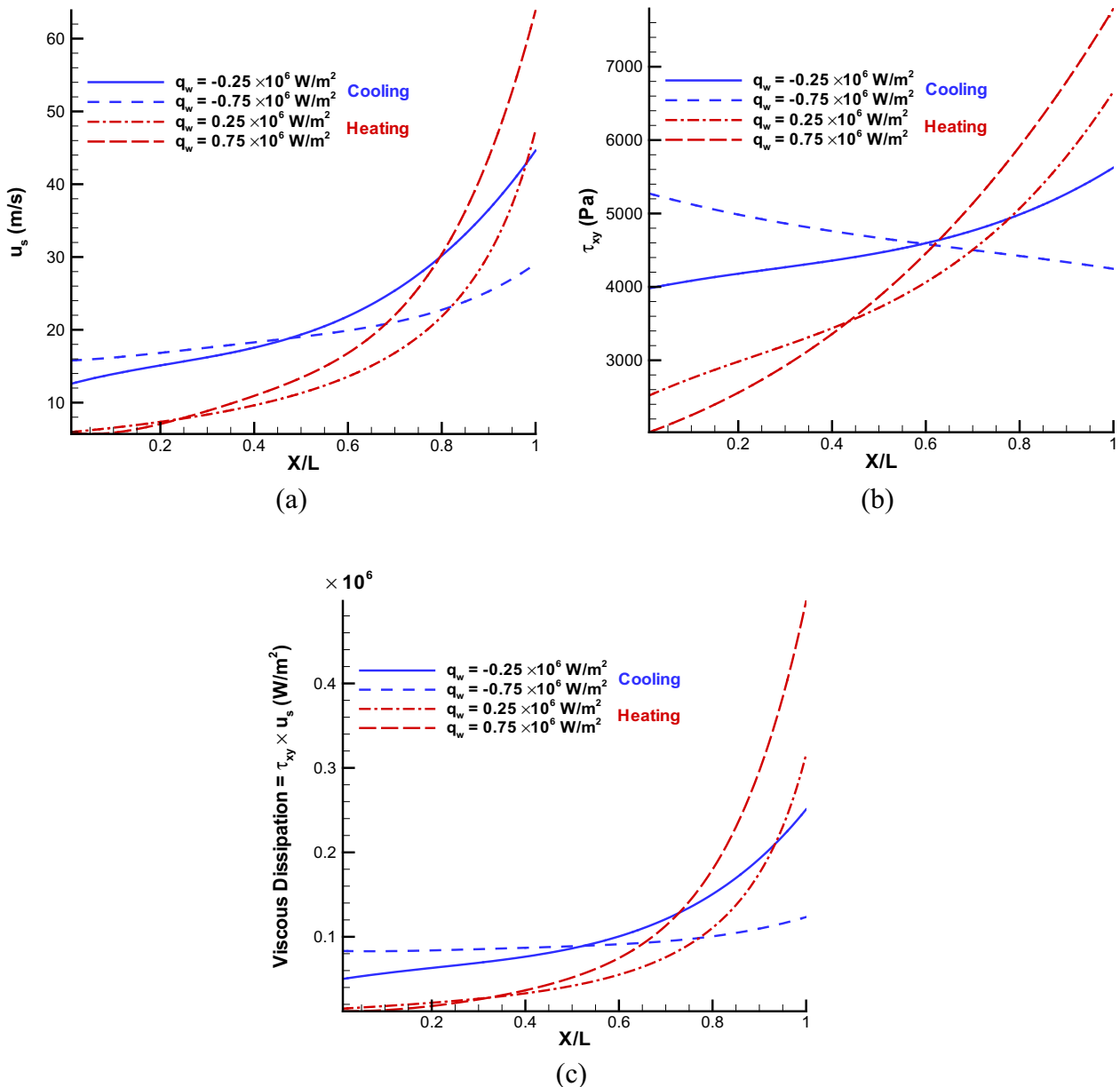


Fig. 4. (a) The slip velocity variation along the channel for different wall heat fluxes, (b) the wall shear stress variation, (c) viscous dissipation near the channel walls.

is conventionally less than the bulk temperature. But at the terminal section of the channel, fluid bulk temperature is greater than the wall temperature. It seems that the wall heats the flow at the end of the channel; however, the specified heat flux is negative, i.e., cooling heat flux. Singularity in the Nu number in Fig. 2 is due to the wall and bulk temperature intersection. In order to provide a numerical explanation for the anomalous temperature distribution in the case of  $q_w = -25 \text{ W/cm}^2$ , the viscous dissipation should be considered.

Hong and Asako [20] physically explained that when there is a slip, the shear work due to the slip at the wall acts as the heat flux in the form of  $\tau_{xy} \times u_s$  from the wall. This term indicates that the effect of viscous dissipation always behaves like a heat source, i.e., heat generation made by the shear stress ( $\tau_{xy}$ ) is usually considerable as the shear stress is considerable at low Reynolds micro/nano flows. The effect of the viscous dissipation depends on whether the walls are being cooled or heated. Fig. 4(a) shows the slip velocity ( $u_s$ ) distribution along the channel. The slip velocity in the DSMC simulations is obtained using the following formula;

$$u_s = \frac{\sum \left( \frac{m}{|v_p|} u_p \right)}{\sum \left( \frac{m}{|v_p|} \right)} \quad (9)$$

where  $|v_p|$  is the absolute value of the normal velocity and  $u_p$  is the velocity magnitude.

At the continuum regime, shear stress is proportional to the velocity gradient ( $\partial u/\partial y$ ) across the walls and viscosity coefficient ( $\mu$ ). In the DSMC simulations, shear stress is obtained as follows:

$$\tau_{xy} = \frac{1}{t_s A} \sum m (V_t^i - V_t^r) \quad (10)$$

where  $t_s$ ,  $A$ ,  $V_t$  are sampling time, area and tangential velocity after and before reflection from the wall, respectively. Fig. 4(b) indicates the shear stress distribution at the walls along the channel. The velocity gradient increases along the channel due to increase in the flow rarefaction. The gas viscosity depends on the fluid temperature and increases (/decreases) in the case of hot (/cold) walls along the channel. In all cases, the shear stress increases along the channel except case 4. In this case, gas viscosity decreases more than the increase in the velocity gradient and this leads to a decrease in the shear stress. Fig. 4(c) shows the viscous dissipation along the channel. The viscous dissipation increases along the channel in all cases. The magnitude of viscous dissipation is the same as the order of wall heat fluxes. It could be concluded that the effect of viscous dissipation on the heat transfer of the micro/nanochannel must be considered simultaneously with the wall heat flux. In the case of cooling boundary condition, shear work decreases the effect of cooling wall heat flux. This could be the reason of wall and bulk temperature intersection in case 3, i.e.,  $q_w = -25 \text{ W/cm}^2$ .

Thermal patterns and gaseous heat transfer direction of the channel have been discussed through this section under constant wall heat flux condition. Heat flux vector in the DSMC method is obtained from the following relations [10]:

$$\begin{aligned} q_x &= \frac{1}{2} \rho \overline{c^2 u'} + n \overline{\varepsilon_{\text{int}} u'} \\ q_y &= \frac{1}{2} \rho \overline{c^2 v'} + n \overline{\varepsilon_{\text{int}} v'} \end{aligned} \quad (11)$$

where  $c'$  is the molecular (or thermal) velocity vector with the magnitude of  $c'$  and  $\varepsilon_{\text{int}}$  is the internal energy of a single molecule.  $n$ ,  $\rho$ ,  $u'$ ,  $v'$  are the number density, mass density and components of velocity  $c'$ , respectively. The effect of viscous dissipation is obvious in contours presented in Fig. 5. This figure shows the heat flux lines

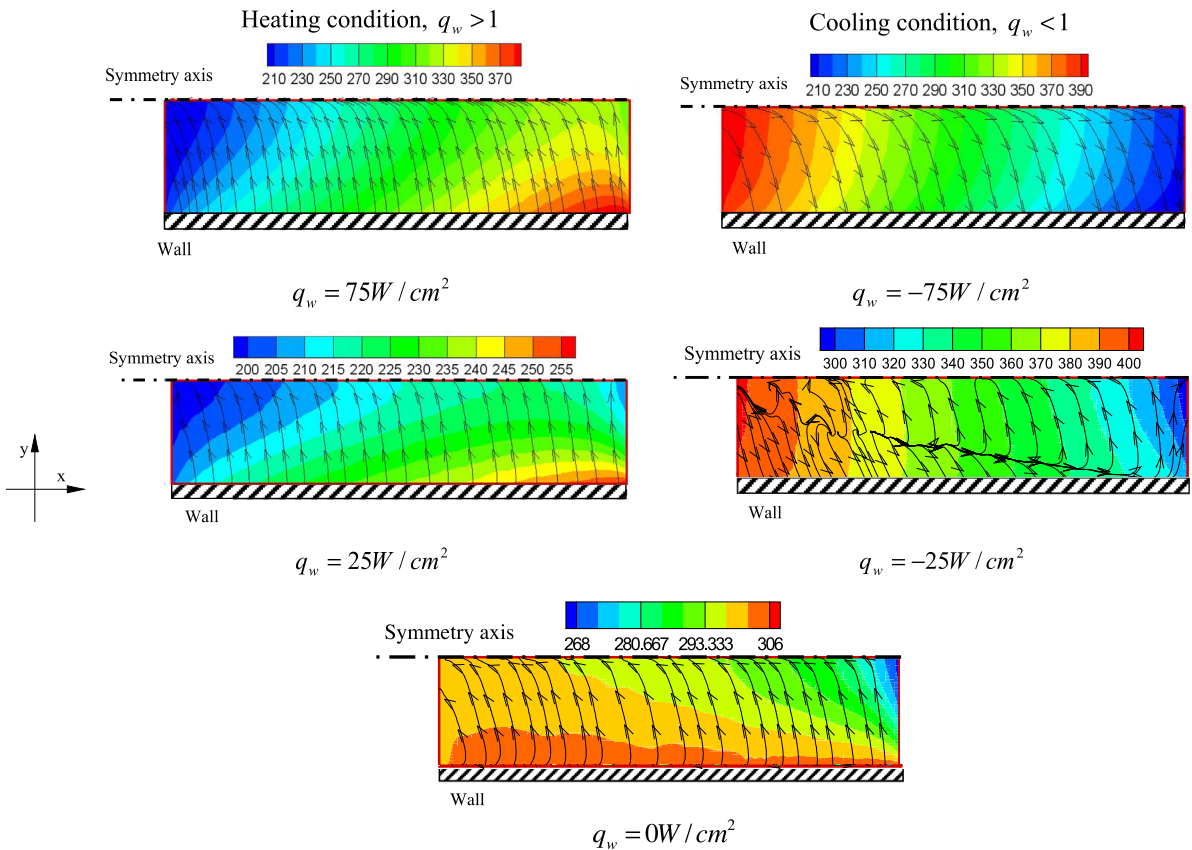


Fig. 5. Heat flux lines overlaid on temperature contours for different wall heat flux cases.

overlaid on temperature contours. According to the temperature contours, there is a significant drop in the temperature field at the outlet, particularly for the cases of heating. This can be attributed to the expansion cooling near the outlet. Based on heat flux lines, an interesting heat flow pattern is observed in the transverse ( $y$ ) direction in the case of  $q_w = -25 \text{ W/cm}^2$ . While cooling is applied to the walls, at the terminal section of the channel, the walls heat the flow, and heat flux lines move in flow direction, i.e., heating occurs.

As it is known, the main driving mechanism for the heat transfer from the wall to the fluid is the temperature difference between the wall and the fluid. When there is a velocity slip, the viscous dissipation operates as a heat transfer mechanism. In other words, in the slip regime, the main mechanisms of the heat transfer are the temperature difference and the viscous dissipation simultaneously. In the case of heating condition, the viscous dissipation enhances the heat transfer rate and increases the positive heat flux. As is clear in heating condition, heat flux lines always stream from the wall toward the gas flow. But in the cooling condition, there is a competition between the cooling heat flux and the viscous heating. Where the cooling wall heat flux is greater than the viscous heating, the heat flux lines move toward the wall. Fig. 4 shows that the viscous dissipation increases along the channel. At the terminal section of the channel, the viscous heating may overcome the cooling wall heat flux. Fig. 4 indicates that in the case of  $q_w = -25 \text{ W/cm}^2$ , the viscous dissipation is at the order of wall heat flux. In this figure, the bifurcation of heat flux lines is due to the different nature of the viscous heating and the cooling wall heat flux. It is noteworthy that the net heat flow direction along the centerline is mainly from a low temperature region to a high temperature region. This counter-gradient heat transfer cannot be predicted by the Navier–Stokes equations [21]. The counter gradient heat flux phenomenon was observed in the cavity geometry as well [21,22].

## 6. Conclusion

The effects of viscous dissipation due to the slip velocity on non-equilibrium heat transfer in a pressure driven micro/nanochannel is discussed under constant wall heat flux condition. The DSMC results show that shear stress on the walls significantly affects all aspects of the flow behavior and heat transfer through micro/nano channel such as heat flux rates. The results indicated that the magnitude of viscous dissipation is in the same order as the order of the wall heat flux and could not be neglected. Therefore, in these cases, both of the viscous dissipation and flow rarefaction must be considered simultaneously to predict heat transfer behavior. Viscous dissipation enhances heat transfer in the case of heating condition and decreases heat transfer rates in the case of cooling condition. In the case of low cooling heat flux, the walls may heat the flow if the viscous dissipation overcomes the cooling wall heat flux. We also investigated the counter gradient heat flow phenomenon appearing in the case of low cooling wall heat fluxes.

## Conflict of interest

None declared

## References

- [1] R. Inman, Laminar slip flow heat transfer in a parallel plate channel or a round tube with uniform wall heating, NASA Technical Note D-2393, 1964.
- [2] K. Hooman, A superposition approach to study slip-flow forced convection in straight microchannels of uniform but arbitrary cross-section, *Int. J. Heat Mass Transfer* 51 (2008) 3753–3762.
- [3] M. Miyamoto, W. Shi, Y. Katoh, J. Kurima, Choked flow and heat transfer of low density gas in a narrow parallel-plate channel with uniformly heating walls, *Int. J. Heat Mass Transfer* 46 (2003) 2685–2693.
- [4] H.E. Jeong, J.T. Jeong, Extended Graetz problem including streamwise conduction and viscous dissipation in microchannel, *Int. J. Heat Mass Transfer* 49 (2006) 2151–2157.
- [5] O. Aydin, M. Avci, Analysis of laminar heat transfer in micro-Poiseuille flow, *Int. J. Therm. Sci.* 46 (2007) 30–37.
- [6] A. Sadeghi, M.H. Saidi, Viscous dissipation and rarefaction effects on laminar forced convection in microchannels, *ASME J. Heat Transfer* 132 (2010) 072401.
- [7] J. Sheela-Francisca, C.P. Tso, Viscous dissipation effects on parallel plates with constant heat flux boundary conditions, *Int. Commun. Heat Mass Transfer* 36 (2009) 249–254.
- [8] N.G. Hadjiconstantinou, Dissipation in small scale gaseous flows, *J. Heat Transfer* 125 (2003) 944–947.
- [9] S. Colin, Gas microflows in the slip flow regime: a critical review on convective heat transfer, *J. Heat Transfer* 134 (2012) 020908.
- [10] G.A. Bird, *Molecular Gas Dynamics and the Direct Simulation of Gas Flows*, Oxford Science, Oxford, UK, 1994.
- [11] H. Akhlaghi, E. Roohi, S. Stefanov, A new iterative wall heat flux specifying technique in DSMC for heating/cooling simulations of MEMS/NEMS, *Int. J. Therm. Sci.* 59 (2012) 111–125.
- [12] H. Akhlaghi, M. Balaj, E. Roohi, Mass flow rate prediction of pressure-temperature-driven gas flows through micro-/nanoscale channels, *Continuum Mech. Thermodyn.* 26 (2014) 67–78.
- [13] H. Akhlaghi, M. Balaj, E. Roohi, Hydrodynamic behaviour of micro/nanoscale Poiseuille flow under thermal creep condition, *Appl. Phys. Lett.* 103 (2013) 073108.
- [14] M. Balaj, E. Roohi, H. Akhlaghi, R.Sh. Myong, Investigation of convective heat transfer through constant wall heat flux micro/nano channels using DSMC, *Int. J. Heat Mass Transfer* 71 (2014) 633–638.
- [15] H. Akhlaghi, M. Balaj, E. Roohi, A through study on thermal mass flux of rarefied flow through micro/nanochannels, *Appl. Phys. Lett.* 104 (7) (2014) 073109.
- [16] H. Akhlaghi, M. Balaj, E. Roohi, K. Dadzie, Effects of wall heat transfer on the hydro/thermal behavior in micro/nanochannels using DSMC, *Phys. Fluids* 26 (9) (2014) 092002.
- [17] H.A. Hassan, D.B. Hash, A generalized hard-sphere model for Monte Carlo simulation, *Phys. Fluids A* 5 (1993) 738–744.
- [18] M.N. Macrossan,  $\mu$ -DSMC: a general viscosity method for rarefied flow, *J. Comput. Phys.* 185 (2003) 612–627.
- [19] M. Balaj, H. Akhlaghi, E. Roohi, Rarefied gas flow behavior in micro/nanochannels under specified wall heat flux, *Int. J. Mod. Phys. C*, accepted, <http://dx.doi.org/10.1142/S0129183115500874>
- [20] C. Hong, Y. Asako, Some considerations on thermal boundary condition of slip flow, *Int. J. Heat Mass Transfer* 53 (2010) 3075–3079.
- [21] B. John, X.J. Gu, D.R. Emerson, Nonequilibrium gaseous heat transfer in pressure-driven plane Poiseuille flow, *Phys. Rev. E* 88 (2013) 013018.
- [22] A. Mohammadzadeh, E. Roohi, H. Niazmand, S. Stefanov, R.Sh. Myong, Thermal and second-law analysis of a micro- or nanocavity using direct-simulation Monte Carlo, *Phys. Rev. E* 85 (2012) 056310.